


Formability investigation of a thin-wall part of double curvature using an integrated reverse engineering environment

Yunxiang Wang , Kuang-Hua Chang  and Peter G. Staub 

The University of Oklahoma, USA

ABSTRACT

An integrated reverse engineering (RE) environment composed of modeling, forming simulation, tooling design and manufacturing, and forming operation was employed to solve an existing problem, in which a thin-wall part of double curvature was not able to be physically formed without tearing and wrinkle after numerous attempts at a logistics center. This paper focuses on the formability study of this challenging part using the newly established RE environment. Forming simulation was heavily employed to explore a narrow window that ensures a successful part forming by investigating blank shape design and understanding the material flow in forming. A key factor that ensures a successful part without tearing or wrinkle was clearly suggested by forming simulations. A physical forming process that incorporates such a factor was implemented at shop floor, which produced an accurate part without tearing and wrinkle for the first time after numerous attempts. Lessons learned are presented and the feasibility of bringing simulation to the shop floor at the logistics center is discussed.

KEYWORDS

Sheet metal forming; numerical simulation; MRO (maintenance; repair; and overhaul); aging systems

1. Introduction

Logistics centers face major challenges in maintaining weapon systems originally designed half a century ago. These weapon systems are approaching or have already reached the end of their intended service lives. For some time, logistics centers have adopted various reverse engineering (RE) approaches that replicate original parts from physical samples. These approaches have provided some success in supporting logistics centers to accomplish its MRO (maintenance, repair, and overhaul) missions. In recent years, some logistics centers have attempted to accelerate the process by implementing an aggression of modern scanning devices with surface construction and solid modeling technology [4].

In manufacturing, some of the technology, process, and equipment, initially employed are outdated, and vendors discontinued part supplies to logistics centers due to numerous factors, such as environmental concerns. In addition, maintaining fleets of aging systems of small quantities only requires small number of parts, which severely narrows the options of viable manufacturing methods and often leads to no-bid after a prolonged acquisition process.

Several product and process re-engineering ideas were proposed to logistics centers. Among them is an

integrated reverse engineering environment that supports the process design and manufacturing of sheet metal parts. Such a system composed of modeling, forming simulation, tooling design and manufacturing, and forming operation has recently been developed and implemented at a logistics center [5]. This integrated environment was employed to solve an existing problem, in which a thin-wall part of double curvature was not able to be physically formed without tearing and wrinkle after numerous attempts.

Prior to the advent of simulation tools, the design of sheet forming process depends on the experience of skillful engineers. Since potential forming defects for geometrically complicated parts are difficult to foresee at early design stage, the blank shape, die face geometry and essential process parameters such as binder force (blank holder force) are usually determined through a tedious and expensive trial-and-error loop. If the part is not formed successfully with the initial design, it requires much time to make adjustment to the process, resulting in a long development cycle, not to mention the high cost of repeatedly correcting the tooling surface.

During the last decade, numerical simulation based on finite element method (FEM) has been increasingly applied in modeling sheet metal forming processes.

Many commercial software packages, such as AutoForm (www.autoform.com), Pam-Stamp (www.esi-group.com) and DynaForm (www.eta.com), have been developed to support the tooling and process designs of various sheet forming applications. These software tools provide engineers with means to validate the process design and make necessary changes before expensive tooling is manufactured, reducing the reliance on trial-and-error. Moreover, they offer the capabilities of blank shape design, die face design, and springback compensation, which contribute to a more effective and efficient experience of producing sheet metal parts. An evaluation of commercially available sheet forming simulation software can be found in [5].

One concern about the current forming simulation technology is whether it is practical in supporting the process design and manufacturing of actual sheet metal parts at the logistics center, especially for challenging ones. Certainly, the most effective and direct way of validating a forming simulation tool is through experiments, or in other words, by comparing the result of numerical simulation to physical forming. A few technical investigations such as [7,8,12] have been reported in respect of applying sheet forming simulation to industrial cases. It has been shown in these studies that commercial simulation tools are capable of predicting physical forming results with acceptable accuracy, and can help in solving problems such as tearing and springback. An integrated CAD/CAE/CAM system was reported in [10,11] to support sheet metal forming of automotive parts and mobile phone components, and was proven to be useful in reducing development cycle, saving cost, and improving product quality. However, much of the literature has been focused on parts with existing die design that needs only minor modifications to achieve a successful forming.

In this paper, formability study is carried out using the newly established RE environment for a challenging sheet metal part that was not able to be physically formed after numerous attempts. In addition to the complex part geometry, challenges also include unknown material and process parameters, the absence of previous die design, as well as the restriction in process design due to the existing forming facility at the shop floor. With the simulation tool integrated in the system, numerical forming analysis can be employed to understand material flow that facilitates the exploration of a narrow forming window for the part. The design of both the die face and the blank shape can be constantly updated according to simulation results. The forming process simulated can be validated at the shop floor to demonstrate the benefit of the integrated RE environment.

To facilitate the discussion, we first briefly introduce the RE environment in Section 2. Section 3 reviews basic

theories regarding sheet forming simulation. The part to be studied, as well as the challenges to be overcome, will be discussed in Section 4. Section 5 presents details of the formability study, including die face construction, blank design, forming simulation, tooling design and manufacturing, and process validation. Lessons learned from the current study are given in Section 6. Conclusions and future tasks are discussed in Section 7.

2. The integrated reverse engineering system

The logistics center is currently employing various software tools and equipment for the design and manufacturing of sheet metal parts. These tools and equipment include scanners that capture part geometry for reverse engineering, software that supports constructing parametric solid models of the parts, production forming equipment, and CNC mills that machine the tools. An evaluation of commercially available sheet forming simulation software [5] has been carried out based on criteria reflecting the needs of the logistics center. Although the tools, equipment, and manufacturing processes at the center have been fully integrated, the selected forming simulation tool has not been fully validated.

An integrated reverse engineering environment that supports design and manufacturing of sheet metal parts, as depicted in Fig. 1, has recently been developed [5]. This environment supports reverse engineering parts from physical samples, conducting forming simulation, selecting adequate forming operation, creating die design, machining dies, and carrying out sheet metal forming for part production. Overall, this system aims at streamlining design and manufacturing workflow, maximizing the benefits of the tools and equipment, improving productivity and supporting cost-effective productions at the logistics center. As can be seen from Fig. 1, the effectiveness of sheet forming simulation is critical to the success of the integrated system. In this paper, we present the validation of the forming simulation tool incorporated in the RE environment through the formability study of a challenging sheet metal part.

3. Basic theories

Formability is the capability of sheet metal to undergo plastic deformation to a given shape without defects such as tearing and wrinkling. The formability of a sheet metal part is a complex characteristic that depends not only on the properties of the blank material but also on the sheet forming process. Currently, the most popular means for evaluating sheet metal formability is the forming limit diagram (FLD), which has been frequently used in failure diagnosis of sheet forming processes and

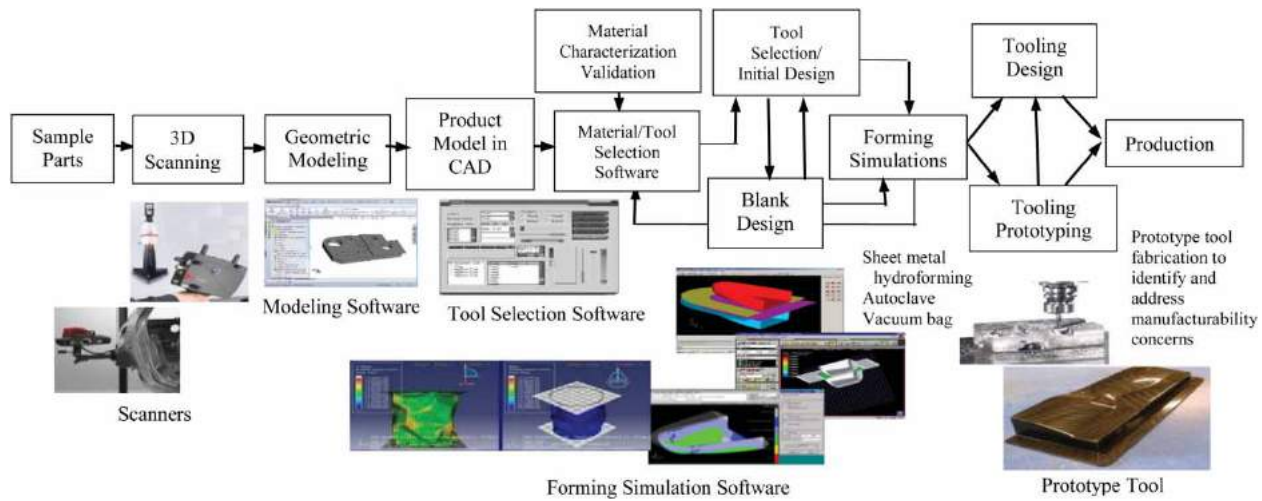


Figure 1. The integrated reverse engineering environment.

has been implemented in most sheet forming simulation software.

As illustrated in Fig. 2, a forming limit diagram is divided into different zones by several curves. The vertical and horizontal coordinates correspond respectively to the major and minor strains. At any instant during a forming process, the deformation at each location on the sheet is represented as a point on the forming limit diagram. The formability of the sheet can be evaluated by comparing the positions of these points to the curves. For example, the forming limit curve (FLC) separates the safe and failure zones, in which a strain state above the FLC implies local necking or fracture. On the other hand, the strain points below the -45 degree line that passes through the origin indicate a thickening of the sheet, and hence strong wrinkling tendency. The FLC for a given material can be established by experiments that provide pairs of values of the limit strains ϵ_1 and ϵ_2 obtained for various loading conditions such as equi-biaxial tension, biaxial tension, and uniaxial tension [1]. In general, the goal of the process design of a sheet metal part is to ensure that all strain points fall into the 'safe' window of the FLD.

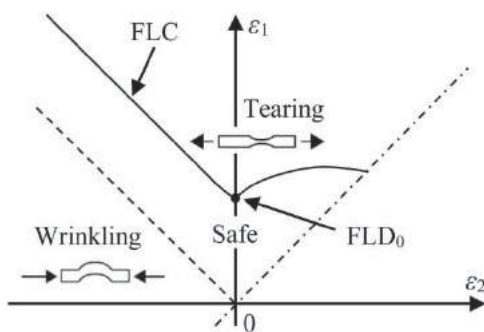


Figure 2. The forming limit diagram.

The key to achieve this is to adequately control the material flow during the forming process. Factors that impact the material flow include blank material properties, process parameters, and the geometric shapes of the blank and tooling.

In sheet forming simulation, the modeling of blank material requires inputs such as the yield criterion and the strain-hardening curve. At present, the most frequently used yield criteria are Hill 1948, Hill 1990, and Barlat 1989 [2], while the strain-hardening behavior can be modeled in different ways such as the Hollomon's law or the Swift-Krupkowski law [6]. In addition, the forming limit curve is determined primarily based on the properties of the blank material such as blank thickness, tensile strength, strength coefficient (K), strain-hardening index (n), and anisotropy coefficients (r_0, r_{45}, r_{90}). For example, in a forming limit diagram, the intersection of the forming limit curve with the vertical axis (noted as FLD_0 in Fig. 2) depends mainly on the strain hardening coefficient and the thickness of the blank [1].

In addition to material properties, the material flow is also determined by the geometry of the tooling surface, the shape of the blank, and process parameters such as friction coefficient, binder force and fluid pressure (for hydroforming). Note that these factors affect the material flow in different ways. For example, the binder force can only control the material flow where the force is applied (usually the binder surface area on the die face), while the friction coefficient takes into effect where the blank is in contact with the tooling. It is also noteworthy that many of the input parameters mentioned above cannot be chosen freely during process design. For example, the yield criteria that can be used often limited to those incorporated in the software, and the blank material is in most cases determined based on the performance of

the finished part with little or no regard to manufacturing. Therefore, as will be discussed later in this paper, the main objective of process design for the sheet metal part is to achieve a successfully forming by systematically adjusting the controllable simulation input parameters, including the die face geometry, blank shape, and blank boundary constraints.

4. Problem descriptions

As shown in Fig. 3a, the studied sheet metal part is a clamp made of Alclad aluminum alloy 2024, with thickness 0.05 in. and key dimensions given in Fig. 3b. As can be seen, forming the part in one shot can be difficult due to the double curvature around the neck and the bends at ears, which may induce both tearing and wrinkles during the forming process. Usually, such a part with delicate geometry requires multiple manufacturing sequences (e.g. bending the ears after the main body is formed). However, since one-shot forming saves both man hours and tooling manufacturing costs, we focused on developing a manufacturing process that forms the part to its desired shape through one single forming operation.

Other than the complex part geometry, additional challenges need to be overcome during the process design. First, the original manufacturing data package of the part was completely missing, indicating that the entire manufacturing process, including the die surface, needed to be built from scratch. Also, since the integrated RE environment was particularly designed for the logistics center, the options available during forming simulation and process design were restricted by the existing facility. For example, no forming equipment currently at the shop floor of the logistics center is capable of applying binder force or supports double action drawing. Moreover, several key process parameters (such as the friction coefficient between tooling and blank) and some of the material properties (such as the strain-hardening index

and anisotropy coefficients) discussed in the previous section were not available. Therefore, these parameters needed to be estimated in our simulations, which will be discussed in the next section.

5. Approaches

Forming simulations were conducted to explore the formability of the part. The die face was designed based on part geometry. The feasibilities of both hydroforming and draw forming were investigated. The finalized draw forming process was implemented at the shop floor with the tooling designed using the RE environment.

5.1. Die face design and forming simulation

According to the evaluation reported in [5], DynaForm (ver. 5.8.1) was chosen as the simulation tool for formability study. The blank material was modeled using DynaForm Material Type 36 (yielding function proposed by Barlat and Lian [2]), which is the most suitable material model available in DynaForm for aluminum alloys. The Swift-Krupkowski law was used for the determination of strain-hardening. Due to the fact that most of the blank material parameters needed for simulation were not available, in simulations, the input properties of Alclad AA2024 were estimated based on experimental data reported in literature, as listed in Table 1.

5.1.1. Hydroforming simulation

The facility at the logistic center supports draw forming and sheet hydroforming, both can be simulated in DynaForm through incremental forming analysis based on the explicit LS-DYNA solver. In this study, hydroforming was investigated first due to its simplicity and the fact that it requires only one tooling block that is more cost effective.

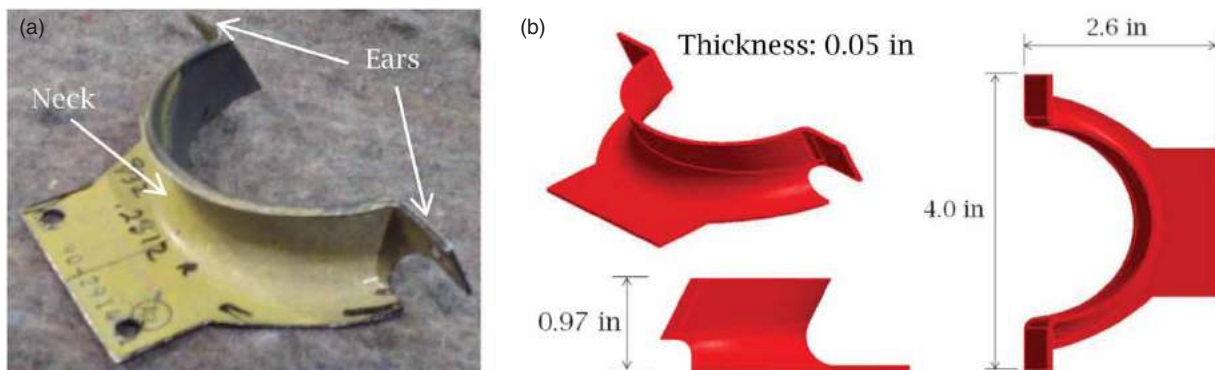


Figure 3. The clamp with double curvature (a) physical sample part, (b) CAD model with key dimensions.

Table 1. Material properties of Alclad AA2024 used in simulation.

Density (g/cc)	Yield Strength (MPa)	Tensile Strength (MPa)	Poisson's Ratio	Young's Modulus (GPa)	Strength Coefficient K (MPa)	Strain-Hardening Index n	Anisotropic Coefficients		
							r_0	r_{45}	r_{90}
2.78	93	200	0.33	73.1	690 ^a	0.16 ^a	0.75 ^b	0.75 ^b	0.75 ^b

^a Reference [9]; ^b Reference [3]

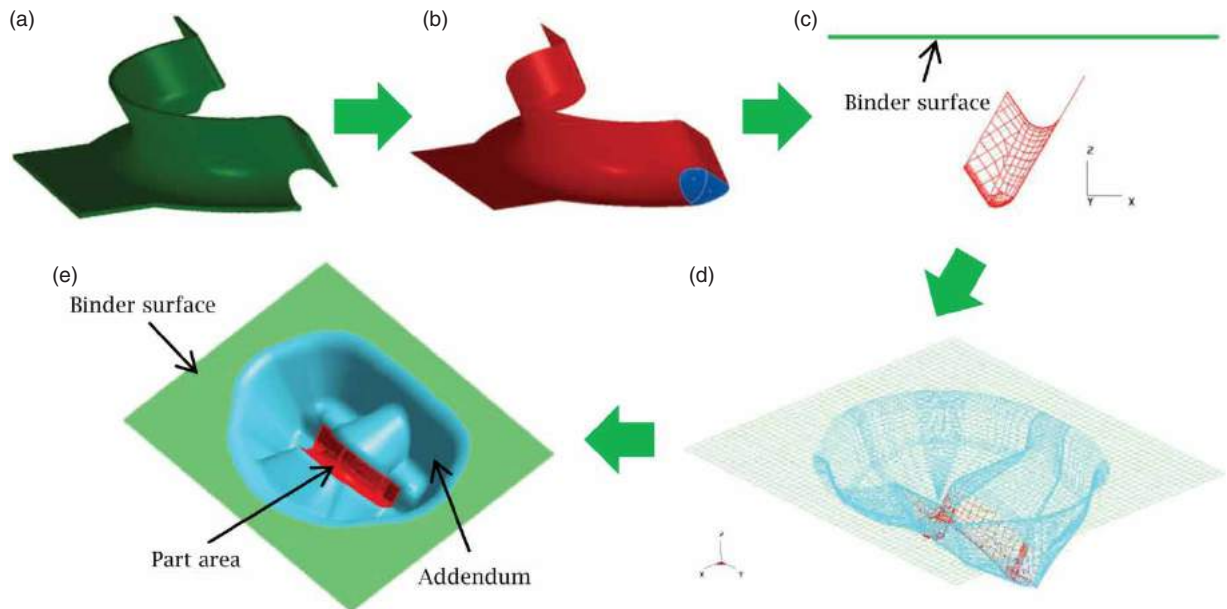


Figure 4. Die face design using the RE environment (a) solid CAD model of part, (b) notches filled and mid-surface extracted, (c) flat binder surface created, (d) addendum created, and (e) complete die face.

Since no previous tooling design of this part was available, the tooling model for forming simulation was established using the RE environment. To avoid unsmooth surface transition during die face creation, the CAD model of the part (Fig. 4a) was first modified in SolidWorks by filling the notches near the ears with loft surfaces (Fig. 4b). Thereafter, the part model was sent to DynaForm, and was carefully oriented to prevent potential undercut. In the meantime, a flat binder surface was created above the part (Fig. 4c). An addendum surface that connects the binder surface and the part area was then automatically generated in DynaForm (Fig. 4d). By trimming the binder surface with the addendum, the complete die face shown in Fig. 4e, which is the combination of the part area, the addendum, and the trimmed binder surface, was obtained.

The setup of the hydroforming simulation with a rectangular blank is illustrated in Fig. 5. Due to geometric symmetry of both the part and the die face, only half of the blank was modeled by imposing a symmetric condition at the symmetry plane. No constraint, however, was applied to the boundary of the blank. The friction coefficient between tooling and blank was set as 0.17 (value provided in DynaForm as 'Standard Aluminum' friction coefficient).

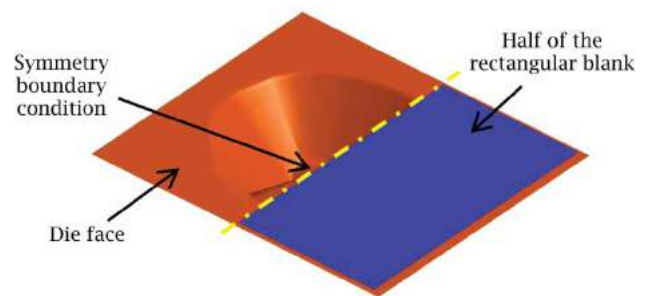


Figure 5. Setup of sheet hydroforming simulation.

Figure 6 shows the hydroforming simulation results, with the boundary of part area highlighted. Colored contour of the forming limit diagram is plotted, in which regions in red, yellow, green, blue, pink, purple, and grey colors denote crack, risk of crack, safe, wrinkle tendency, wrinkle, severe wrinkle, and insufficient stretch, respectively. As can be seen in Fig. 6a, with a rectangular blank, the process was predicted to result in severe tearing at the end of forming. Based on the simulation result, the blank shape was modified and turned into a 'T' shape after several attempts. As shown in Fig. 6b, the T-shaped blank significantly reduced the red area; however, major tearing can still be observed around the deepest location

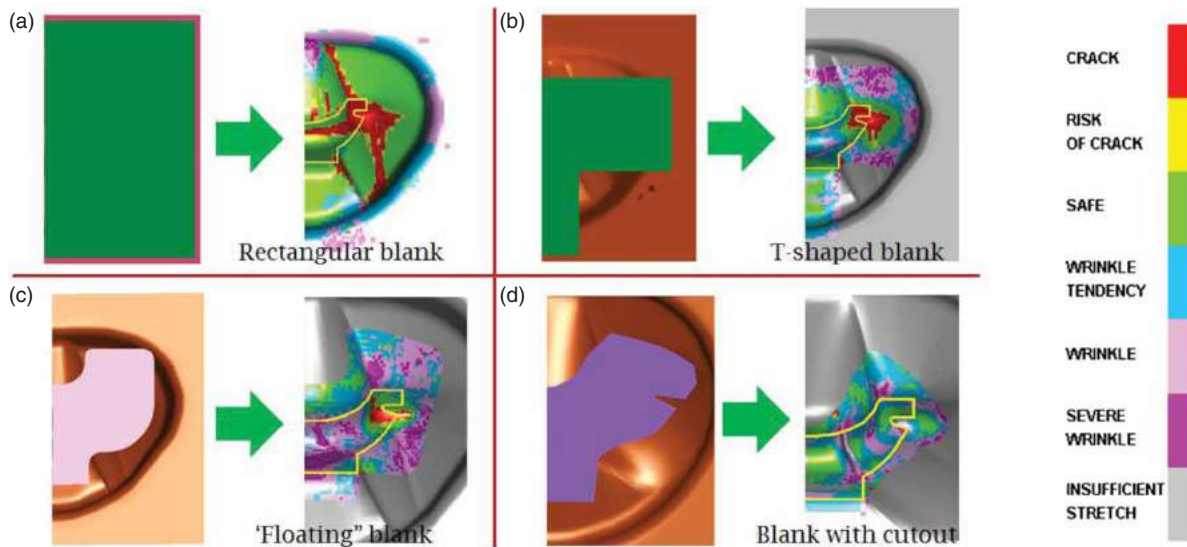


Figure 6. Sheet hydroforming simulation results (top view). Half blank shown due to symmetry. Yellow curves indicate part boundary. (a) Rectangular blank with severe tearing, (b) T-shaped blank with tearing at the deep pockets, (c) floating blank with wrinkles and tearing, and (d) floating blank with cutout leading to severe wrinkles.

of the die pocket. Many other blank designs were tested afterwards, and it was found that the tearing spots on the formed blank could not be further reduced unless, at the beginning of forming, the blank was made ‘floating’ on top of the die without any support to delay the contact of the blank with the die surface (Fig. 6c), which is apparently very difficult if not entirely impossible to implement. By using a ‘floating’ blank with a cut-out shown in Fig. 6d tearing on blank was completely removed; however, the blank material near the neck of the part was severely wrinkled.

In addition to blank shape, the geometry of the die face was adjusted in hope of improving the hydroforming result. Unfortunately, none of these ideas led to an acceptable simulation result. Therefore, it was concluded that hydroforming was not feasible for the part forming. The main reason was due to the high fluid pressure applied in hydroforming, in which material was severely restricted locally once it was in contact with the tooling surface, resulting in insufficient material flow into the deep die cavity, which eventually caused tearing.

5.1.2. Draw forming simulation

Using DynaForm, draw forming simulations were then performed for this part. The die face designed previously for hydroforming was used as the female tool, while the male punch was modeled by copying and offsetting the geometry of the die. Figure 7 illustrates the setup of the draw forming simulation. Due to the limitation of the forming equipment available at the logistics center, binder force could not be implemented. Therefore, as shown in Fig. 7, fixed boundary condition was applied to

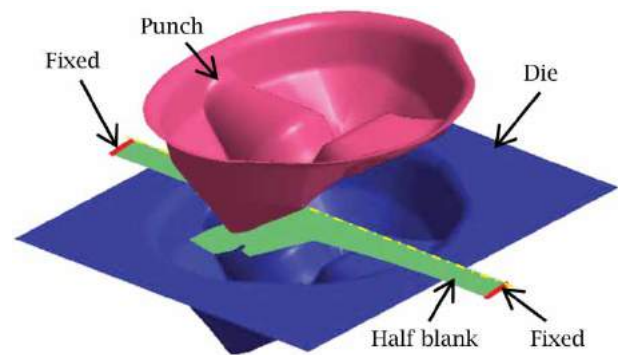


Figure 7. Setup of draw forming simulation.

the blank, i.e., the blank was clamped at both ends. The velocity of punch was set to be 5000 mm/s (196.9 in/s). As with hydroforming, only half of the blank was modeled due to symmetry.

Note that the shape of the blank shown in Fig. 7 was the outcome after numerous unsuccessful blank designs, some of which are shown in Fig. 8. As can be seen, from a rectangular blank (Fig. 8a) to T-shaped blank with steps (Fig. 8b), and finally to a blank with wings (Fig. 8c), unnecessary blank material was gradually removed in order to minimize the contact between blank and tooling surface for achieving a better material flow. Both clamped and free boundary conditions were tested for each blank design. It turned out that while most of the infeasible designs resulted in severe tearing or wrinkling of the blank, a carefully designed blank with wings (Fig. 8c) yielded a relatively promising result as shown in Fig. 9, where the punch is displayed as a wireframe and the part boundary is highlighted in orange.

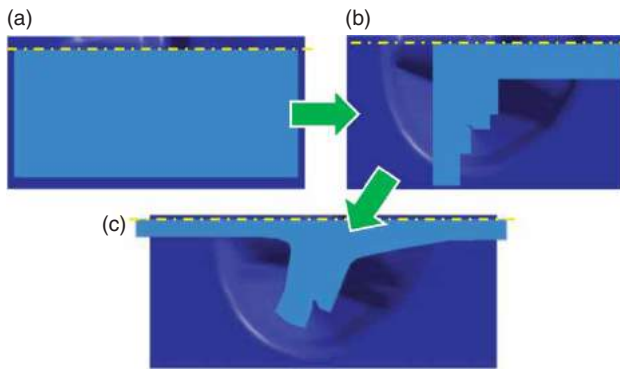


Figure 8. Some of the blank designs explored.

It is clear, however, that the potential problems indicated in Fig. 9, especially the tearing elements that spreads all the way into the part area, were still unacceptable. To reduce tearing, the die surface was smoothed using DynaForm by flattening the sharp steps near the punch opening line (Fig. 10). In the meantime, as shown in Fig. 11, the shape of the blank outline was further

edited for numerous times in order to eliminate tearing zones 1 and 2 in Fig. 9.

The draw forming simulation result with modified die face and blank shape (*Blank Design 1* of Fig. 11) is given in Fig. 12a. Note that tearing zones 3 and 4 disappear due to the smoothed die face, while tearing at Zone 1 has been reduced and kept out of the part boundary. However, since DynaForm is incapable of simulating crack propagation, the result after the onset of tearing was not reliable. As shown in Fig. 12b, the simulation animation for the result shown in Fig. 12a includes a total of 27 frames, while tearing at Zone 1 occurred at Frame 20/27. Apparently, the results after Frame 20 should be ignored regardless of whether the red elements were eventually inside or outside the part area. No tearing should be tolerated in simulation in order to produce a working part without crack.

A simplest way of eliminating tearing is to allow more material flow at both ends of the blank, which can be realized by adjusting the clamping forces. However, if both sides of the blank are allowed to move along the length

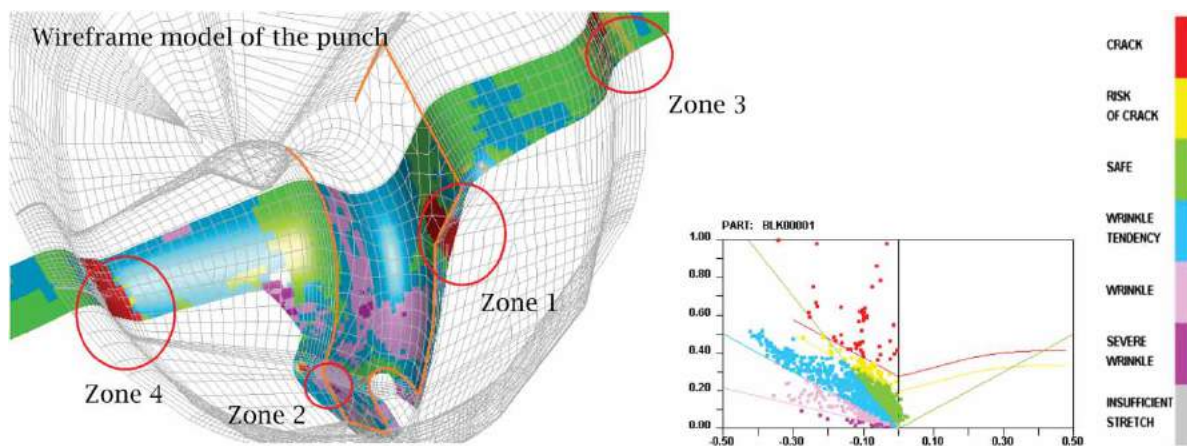


Figure 9. Draw forming simulation result. Part boundary highlighted in orange color.

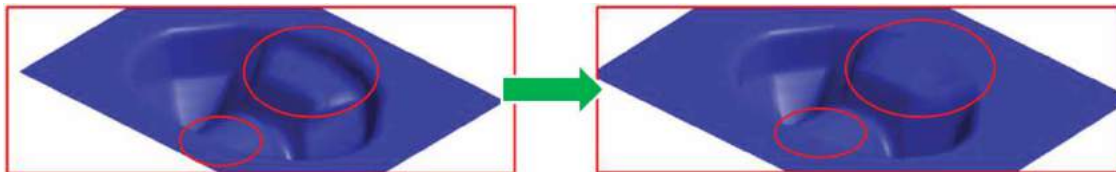


Figure 10. Modifications made to smooth the sharp steps on the die face.



Figure 11. Modifications made to blank shape.

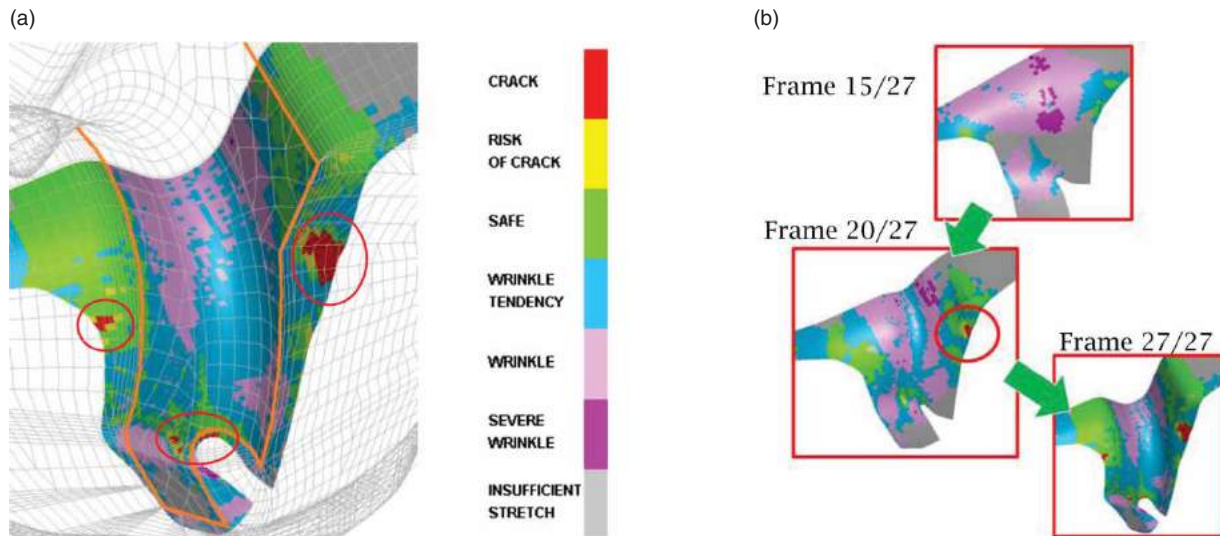


Figure 12. Simulation result with modified die face and blank shape (a) forming simulation at the end, and (b) intermediate animation frames.

direction, the final position of the blank with respect to the die cannot be guaranteed. This is because that in practice the clamping forces are difficult to control precisely. Therefore, the left side of the blank was chosen to be fixed, while the blank material was allowed to flow on the right side with a reduced clamping force. As shown in Fig. 13, the simulation setup was modified to model this scenario, in which the original binder surface was extended, and the fixed boundary condition was replaced by two ‘binders’, one on each side. On the left hand side, a large binder force (5 ton) was applied to mimic a fixed boundary condition, while on the other side the binder force (clamping force during implementation) was adjustable for controlling the material flow. The simulation results with various binder forces on the right are shown in Fig. 14. As can be seen, when the blank was fixed only on the left, major tearing (Zone A) appeared on the other side of the part compared to previous simulations (e.g., Fig. 12a). Moreover, with smaller binder forces, the crack showed

up later in simulation, while tearing in Zone A was significantly reduced due to more material flow from the right. It was also found, however, that the tearing elements in all three zones could not be completely eliminated even by further reducing the binder force to be lower than 0.02 ton; in the meantime, adjusting the friction coefficient had only minimum impact on simulation results.

Since the binder force and boundary constraint could only control the material flow at the two ends of the blank, the shape of the blank was then modified specifically to remove the tearing elements at the particular locations. As shown in Fig. 15, based on the simulation results, the blank outline near Zone A was smoothed; meanwhile, unnecessary material near the neck and the cut-out was removed to minimize the contact between tooling and blank. The simulation result with the modified blank (*Blank Design 2*) and a 0.05 ton binder force is shown in Fig. 16, which indicates no tearing by the end of forming.

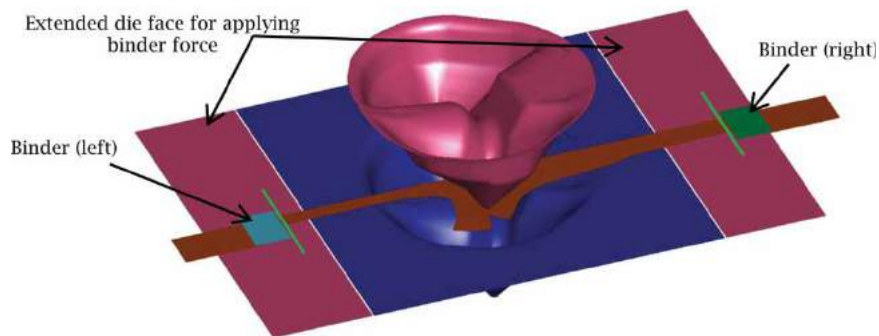


Figure 13. Modified simulation setup with binders.

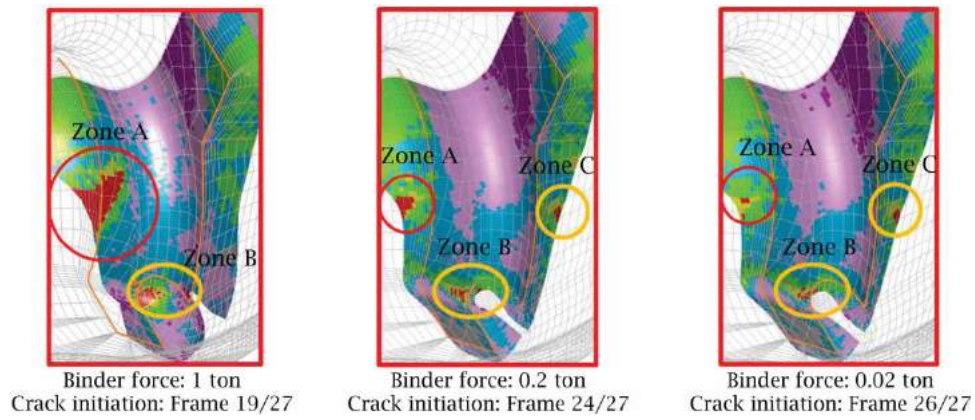


Figure 14. Simulation results with various binder forces.

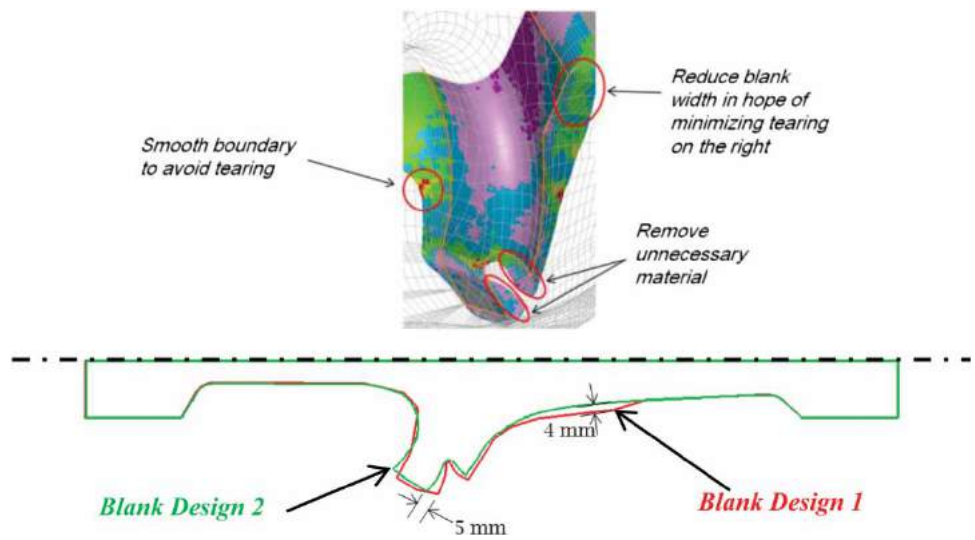


Figure 15. Modified blank design.

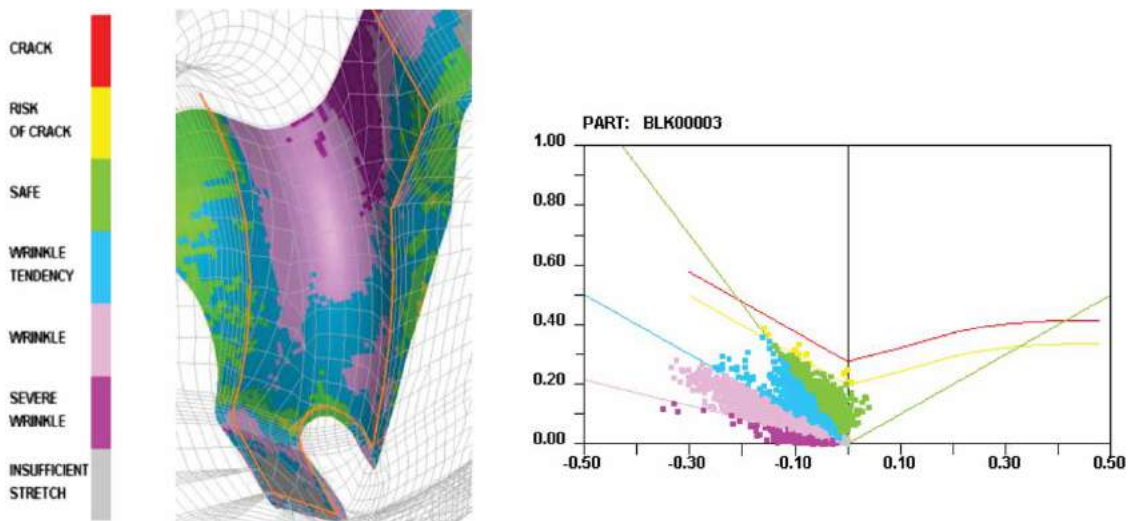


Figure 16. Simulation result with 0.05 ton binder force and Blank Design 2.

It is important to note that as shown in Fig. 14, one factor that all torn blanks shared in common was that the ears were bent early during the process and then dragged by the punch down to the deep pocket of the die, resulting in insufficient material flow from the right, and hence excessive stretch of the blank material on the left of the ears. On the other hand, as shown in Fig. 16, the modified blank (*Blank Design 2*) was able to slide around the tip of the punch without being bent, which contributed to a more evenly distributed material flow. This turned out to be a key factor that ensures a successful forming of the part during shop floor implementation.

5.2. Tooling design and manufacturing

The finalized die face was exported from DynaForm and then imported into SolidWorks for tooling design. The tooling was designed to reflect both the simulations shown in Fig. 12 (with fixed boundary condition and *Blank Design 1*) and in Fig. 16 (with binders and *Blank Design 2*). To implement the ‘fixed’ scenario (Fig. 12), the blank was extended in length direction, and wrapped over the side faces of the die block, as illustrated in Figs. 17a and 17b. Each end of the blank was designed to be

bent three times and hold tightly against the die block with two clamps and twelve bolts in order to avoid slippage during forming. In addition, two shallow slots were cut at the edges of the block, as shown in Fig. 17c, to facilitate the transverse alignment of the blank with tooling. To implement the ‘binder’ scenario, two bolt holes were drilled on the top face of the die block, as shown in Fig. 17d, so that the clamp on the right could be moved to the top face to provide holding force that could be adjusted by tightening up the two bolts at different torque levels. The blank was bent and clamped only on the left side.

Toolpath generation for tooling manufacturing was carried out using Pro/MFG (www.ptc.com) with maximum scallop height of half a thousandth inch. The machined punch and die (cut out of two Kirksite blocks) as well as one of the aluminum clamps are shown in Fig. 18a. Figure 18b shows the implementation of the ‘binder’ scenario.

5.3. Process implementation and validation

A series of forming attempts were conducted on a 300 ton press at the shop floor of the logistics center. The forming setup that led to the result in Fig. 12a (with

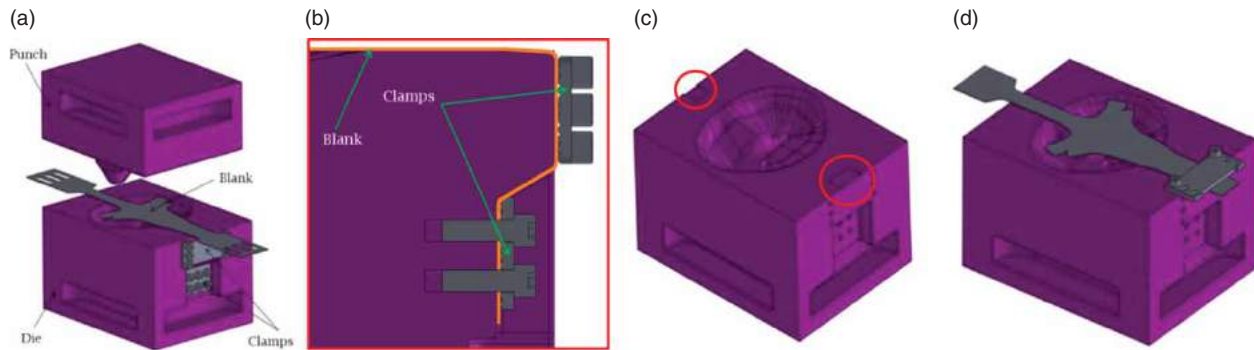


Figure 17. Tooling model designed in SolidWorks (a) positioning of blank, punch, die, and clamps (b) each side of blank is held by two clamps to mimic a fixed boundary condition, (c) shallow slots designed for transverse blank alignment, and (d) setup for the ‘binder’ scenario.

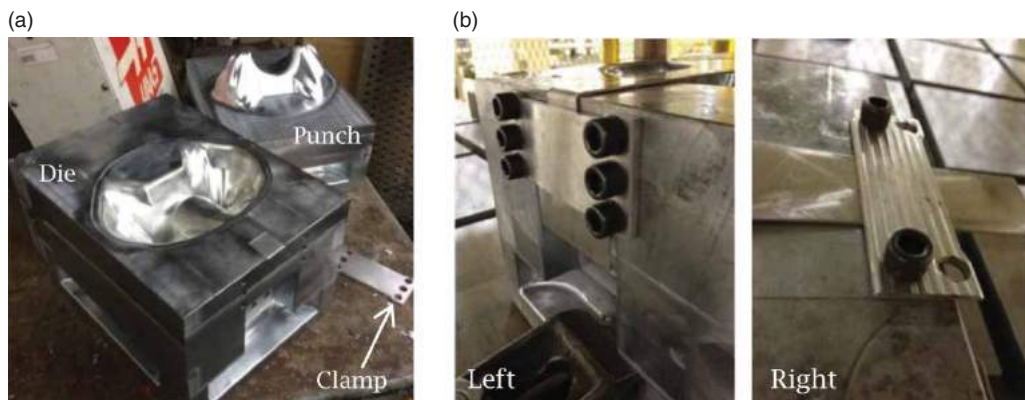


Figure 18. Manufactured tooling blocks (a) punch, die and clamps machined, (b) implementation of the forming scenario with ‘binders’.



Figure 19. Blank formed with fixed boundary condition.

fixed boundary condition and *Blank Design 1*) was implemented first. During the forming process, the blank was broken into two pieces, and, as shown in Fig. 19, the location of tearing was accurately predicted by simulation. The process was then repeated with lubricant and minimized clamping forces on both ends in order to allow more material flow, which resulted in a cracked blank as shown in Fig. 20.

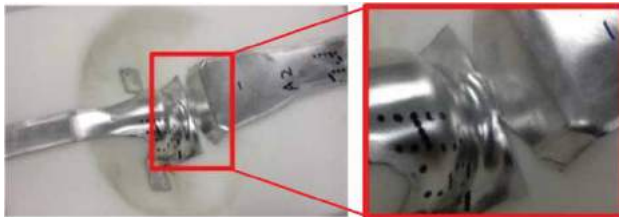


Figure 20. Blank formed with lubricant and loosened clamping forces.

To further verify the accuracy of the forming simulation, a simulation model was established afterwards that attempted to recapture the physical forming scenario shown in Fig. 20. Due to the loosened boundary constraint, the actual blank flowed inward by 3 mm (0.12 in.) and 9 mm (0.35 in.) respectively at the left and right edges at the end of forming (Fig. 21a). Therefore, the forces applied to the two binders shown in Fig. 13 were adjusted to obtain the same material flow in simulation. It was

found that when 2.5 ton and 1.5 ton binder forces were assigned respectively to the left and right binders, the material flow at the moment of tearing initiation (Frame 20/27) matched that observed at the end of physical forming. If it is assumed that during physical forming the material flow at both edges did not increase after the crack started to propagate, the simulation case can be considered as consistent with physical forming in terms of material flow. Under this circumstance, the location of initial tearing measured in this simulation case (43 mm or 1.69 in. from the corner of the cut out) matched well with the physical forming result (41 mm or 1.61 in.), as shown in Fig. 21b. Thus, it was verified quantitatively that DynaForm is capable of predicting the mechanics of physical forming with acceptable accuracy before tearing occurs in simulation.

The simulation setup that led to the result in Fig. 16 was then implemented at the shop floor, in which a 0.05 ton clamping force (bolt force) was applied to the right side of the blank. It turned out that although the simulation predicted no tearing, cracks were observed on the formed blank towards the closure of punch and die. As can be seen from Fig. 22, the location of the crack on the formed blank was consistent with the location of tearing at Zone A shown in Fig. 14. After the first failed part, a few more blanks were formed by adding lubricant between tooling and blank, and at the same time lowering the blank holding force to minimum (bolts finger tighten); however, although smaller, cracks still initiated on blank.

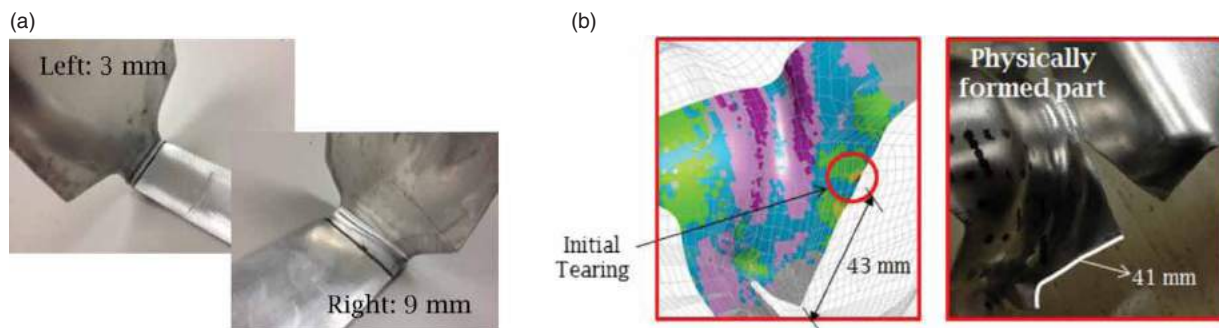


Figure 21. Comparison between simulation and physical forming results (a) material flow on formed blank, and (b) comparison of crack location.

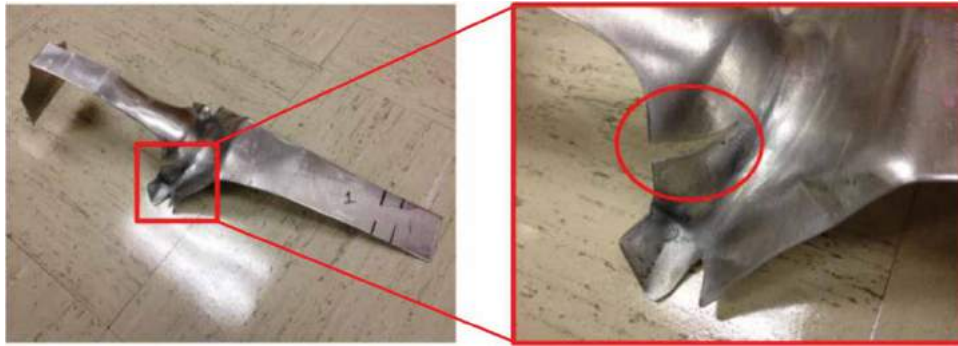


Figure 22. Blank formed by directly implementing the simulation result shown in Fig. 16.

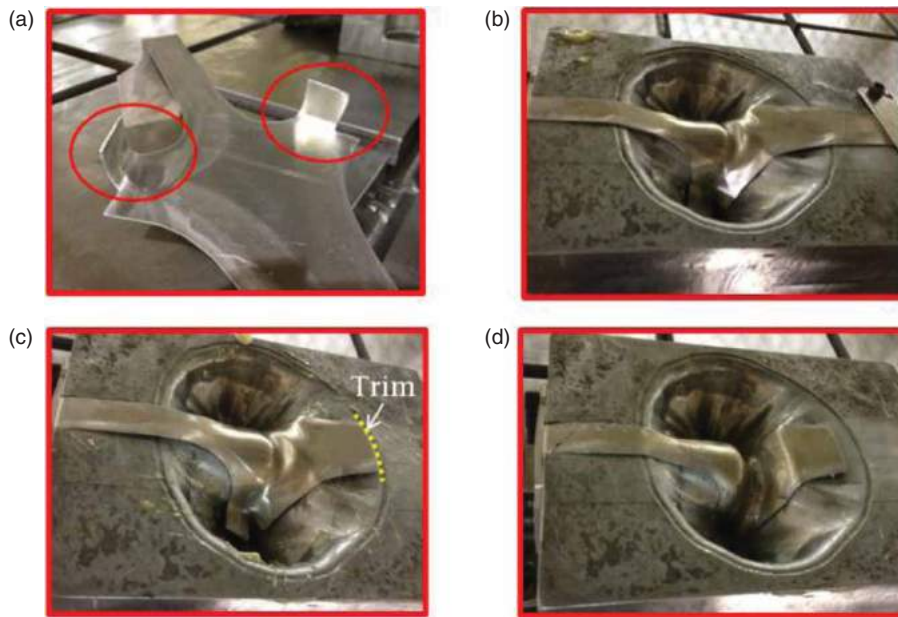


Figure 23. Forming tricks implemented at the shop floor (a) bend the ears in advance, (b) form the blank until the punch is 0.75 in. before closing, (c) trim off the right side of the blank to allow more material flow, and (d) continue forming until die and punch close.

One possible cause of the inconsistency between simulation and actual forming might be the inaccurate input parameters. In simulations, the properties of the blank material were mostly estimated without experimental testing – same for the forming limit curve and the friction coefficient between blank and tooling. Another possible cause was the uncertainty during physical implementation. For example, according to simulation, in some cases the forming result can be sensitive to factors such as blank shape. As has been shown in Fig. 15, a slight adjustment made to the blank outline (a few millimeters) can result in a significant change in forming result (from tearing to no tearing). However, at the shop floor, the blank shape and the binder force applied may not be precise; and more importantly, the alignment of blank may not be able to stay accurate throughout the forming process, which can lead to an inconsistent outcome compared to the simulation result.

Since the simulation result in Fig. 16 could not be physically reproduced with 100% confidence, two forming tricks were implemented based on our findings in simulation. As shown in Fig. 23a, the first trick was to bend the ears beforehand. As observed in simulations (Figs. 14 and 15), the ears on the blank were bent and dragged into the deep pockets, which was believed to be the major cause of tearing on the failed blanks. By bending the ears beforehand, the contact area between the ears and the punch was significantly reduced, which helped the ears to slide away from the tip of the punch, thus avoiding being dragged into the deep pockets. In addition, to maximize the material flow from the right, the forming process was paused at about 0.75 in. before closure. The partially formed blank was taken out of the tooling and trimmed off its right portion to completely remove holding force from the right. The trimmed blank was then brought back to the tooling and the forming was



Figure 24. Successfully formed part (left) with the matching half in yellow color (right).

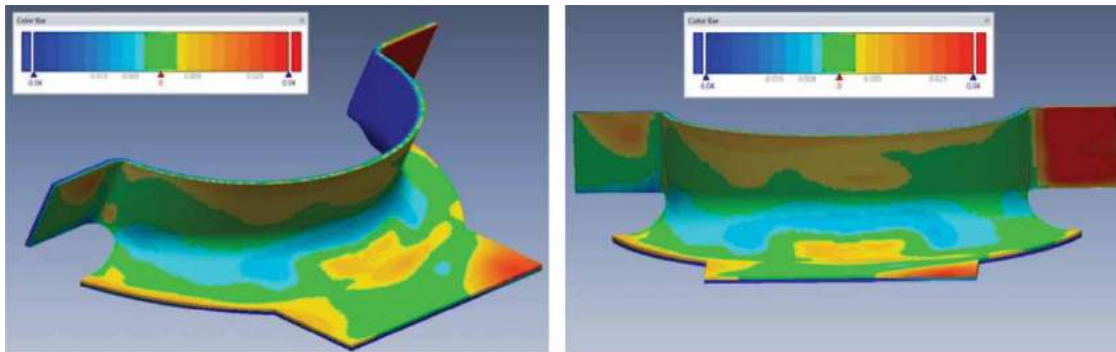


Figure 25. Deviation check for the formed part.

resumed until the punch and die close completely. This process is illustrated in Figs. 23a to 23d.

With the implementation of the two tricks, the ears were able to slide to the right position successfully without being dragged into the deep pockets. A blank was formed to the end with no tearing or wrinkle, producing a working part that fits well with the other half of the fuel line clamp, as shown in Fig. 24. The same forming process was repeated several times and created the same part, which verified the repetitiveness of the process.

The successfully formed part was scanned into computer using ATOS III scanner (www.gom.com/metrology-systems/3d-scanner.html) to be compared with the CAD model for accuracy verification. As shown in Fig. 25, the deviation between the original CAD design and the scanned part was between ± 0.04 in, which satisfied the engineering requirements for the part.

It is worthy of note that workers at the logistics center had spent on this part more than two hundred man-hours at shop floor during the past few years, yet not even one blank was successfully formed, let alone the time and cost spent on tooling design and manufacturing. With the newly established RE environment, however, the majority of the man-hours (less than sixty hours) were spent on blank design, die face design, and forming simulation setup, while only about twenty man-hours were spent at the shop floor before the first successful part was made.

Therefore, it is clear that the RE environment can contribute to a significant time saving in solving challenging cases.

6. Lessons learned

Through the formability study of the fuel line clamp, it has been shown that forming simulation is not only feasible, but also a necessity for sheet metal parts with challenging geometry. The simulation technology provides a reasonable starting point for both process and tooling designs, and meanwhile serves as an excellent guide of physical forming. With advanced simulation tools, engineers are allowed to try different forming processes (e.g., hydroforming, draw forming, stretch forming, etc.), die designs, blank shapes, and binder forces without physically manufacturing expensive tooling and committing effort at the shop floor. Potential forming defects, such as tearing and wrinkling, as well as their fundamental causes, can be detected and resolved at early stage of the design cycle with minimal costs.

On the other hand, it is important not only to use the simulation tool, but also to use it in a correct and effective way. First of all, the interpretation of simulation results is a critical step in simulation-based process design. In our opinion, the simulation technology in the field of sheet metal forming has not been developed to such a level that

it can work completely independent in design process; therefore, simulation results must be carefully examined and fully understood in order to avoid pitfalls and maximize the benefits. A basic knowledge of the mechanics behind sheet forming processes can undoubtedly help engineers make better conclusions and design decisions.

Moreover, inaccurate input parameters may hinder the software from producing realistic predictions. The material properties and process parameters must be carefully measured and calibrated for the blank material; in the meantime, the yielding model, strain-hardening model, and forming limit diagram used in simulation must be explored and validated experimentally in order to ensure an accurate and reliable modeling of material behavior. Furthermore, forming facility and process implemented must be consistent with simulation. For example, the binder force and boundary condition applied in physical forming, or the fluid pressure set up in hydroforming, must be as close as possible to those defined in simulations, so that the predicted forming result can be reproduced during shop floor implementation.

7. Conclusions

In this paper, the formability study of a challenging part using a newly established RE environment has been presented. The forming process designed based on simulation results was validated experimentally through physical forming. It has been shown that forming simulation offers engineers the capability to easily assess the formability of sheet metal parts, which is not only realistic but also effective in solving existing industrial problems. In addition, lessons learned from the case study were summarized, and technical remarks regarding the use of simulation tools have been identified.

With forming simulation incorporated into the RE environment, tooling design and manufacturing of sheet metal parts at the logistics center can be more productive and cost-effective by minimizing the need of traditional trial-and-error loops. Certainly, more needs to be done in order to take full advantage of the simulation tool. For example, material properties of blank materials frequently used at the logistics center need to be accurately measured; also, it is necessary to develop a binder system on top of the current forming facility so that a better control of material flow can be achieved in draw forming.

Acknowledgement

The authors acknowledge the support of engineers and shop floor workers at the logistics center. Their help is highly appreciated.

ORCID

Yunxiang Wang  <http://orcid.org/0000-0002-4446-1832>

Kuang-Hua Chang  <http://orcid.org/0000-0003-0156-0221>

Peter G. Staub  <http://orcid.org/0000-0002-5087-4625>

References

- [1] Banabic, D.: *Sheet Metal Forming Processes*, 2010, ISBN: 978-3-540-88113-1.
- [2] Barlat, F.; Lian, J.: Plastic Behavior and Stretchability of Sheet Metals. Part I: A Yield Function for Orthotropic Sheets under Plane Stress Conditions, *International Journal of Plasticity*, 5, 1989, 51–66. [http://dx.doi.org/10.1016/0749-6419\(89\)90019-3](http://dx.doi.org/10.1016/0749-6419(89)90019-3)
- [3] Bressan, J.D.; Leacock, A.G.: Influence of Pre-strain on the Formability of 2024 Aluminum Alloy, *International Journal of Material Forming*, 2(1), 2009, 475–478. <http://dx.doi.org/10.1007/s12289-009-0587-5>
- [4] Chang, K.H.; Chen, C.: 3D Shape Engineering and Design Parameterization, *Computer-Aided Design & Applications*, 8(5), 2011, 681–692. <http://dx.doi.org/10.3722/cadaps.2011.681-692>
- [5] Chang, K.H.; Wang, Y.: Evaluation of Sheet Forming Simulation for an Integrated Reverse Engineering System, *Computer-Aided Design & Applications*, 10(5), 2013, 767–777. <http://dx.doi.org/10.3722/cadaps.2013.767-777>
- [6] Degarmo, E.P.; Black, J.T.; Kohser, R.A., *Materials and Processes in Manufacturing* (9th ed.), Wiley, 2003
- [7] Duan, L.; Miao, D.; Cai, Y.; Qu, Z.; Li, Z.: Research on Numerical Simulation for Automotive Panel Forming and Spring-back Based on DynaForm, *Measuring Technology and Mechatronics Automation (ICMTMA)*, 3, IEEE, 2011, 55–58. <http://dx.doi.org/10.1109/ICMTMA.2011.585>
- [8] Gantar, G.; Pepelnjak, T.; Kuzman, K.: Optimization of Sheet Metal Forming Processes by the Use of Numerical Simulations, *Journal of Materials Processing Technology*, 130–131, 2002, 54–59. <http://dx.doi.org/10.1016/j.jmatprotec.2007.06.018>
- [9] Kalpakjian, S.; Schmid, S.: *Manufacturing Processes for Engineering Materials* (5th Edition), Prentice Hall, NJ, 2007.
- [10] Lin, B.T.; Kuo, C.C.: Application of an Integrated CAD/CAE/CAM System for Stamping Dies for Automobiles, *International Journal of Advanced Manufacturing Technology*, 35, 2008, 1000–1013. <http://dx.doi.org/10.1007/s00170-006-0785-y>
- [11] Lin, B.T.; Kuo, C.C.: Application of an Integrated RE/RP/CAD/CAE/CAM System for Magnesium Alloy Shell of Mobile Phone, *Journal of Materials Processing Technology*, 209, 2009, 2818–2830. <http://dx.doi.org/10.1016/j.jmatprotec.2008.06.032>
- [12] Zhang, D.H.; Bai, D.P.; Liu, J.B.; Guo, Z.; Guo, C.: Formability Behaviors of 2A12 Thin-wall Part Based on DYNIFORM and Stamping Experiment, *Composites: Part B*, 55, 2013, 591–598. <http://dx.doi.org/10.1016/j.compositesb.2013.07.001>